Dalton Transactions

PAPER

View Article Online
View Journal | View Issue

Open Access Article. Published on 02 April 2015. Downloaded on 4/3/2026 6:59:41 AM.
This article is licensed under a Creative Commons Attribution 3.0 Unported Licence.

Cite this: *Dalton Trans.*, 2015, **44**, 10177

Turning a "useless" ligand into a "useful" ligand: a magneto-structural study of an unusual family of Cu^{II} wheels derived from functionalised phenolic oximes†

Jamie M. Frost,[a] Robert J. Stirling,[a] Sergio Sanz,[a] Nidhi Vyas,[b] Gary S. Nichol,[a] Gopalan Rajaraman*[b] and Euan K. Brechin*[a]

Received 3rd March 2015,
Accepted 31st March 2015

DOI: 10.1039/c5dt00884k

www.rsc.org/dalton

While the phenolic oximes (R-saoH$_2$) are well known for producing monometallic complexes of the type [M^{II}(R-saoH)$_2$] with Cu^{II} ions in near quantitative yield, their derivatisation opens the door to much more varied and interesting coordination chemistry. Here we show that combining the complimentary diethanolamine and phenolic oxime moieties into one organic framework (H_4L_1 and H_4L_2) allows for the preparation and isolation of an unusual family of [Cu^{II}]$_n$ wheels, including saddle-shaped, single-stranded [Cu^{II}_8] wheels of general formula [$Cu_8(HL_1)_4(X)_4$]^n[Y] (when n = 0, X = Cl^-, NO_3^-, AcO^-, N_3^-; when n = 2+ X = $(OAc)_2$/(2,2′-bpy)$_2$ and Y = $[BF_4]_2$) and [$Cu_8(HL_2)_4(X)_4$] (X = Cl^-, Br^-), a rectangular [$Cu_6(HL_1)_4$] wheel, and a heterometallic [$Cu_4Na_2(HL_1)_2(H_2L_1)_2$] hexagon. Magnetic studies show very strong antiferromagnetic exchange between neighbouring metal ions, leading to diamagnetic ground states in all cases. DFT studies reveal that the magnitude of the exchange constants are correlated to the Cu–N–O–Cu dihedral angles, which in turn are correlated to the planarity/puckering of the [Cu^{II}]$_n$ rings.

Introduction

In the early days of molecular magnetism low nuclearity complexes containing Cu^{II} ions were the focus of intense research efforts by synthetic chemists and theoreticians.[1–5] The ease of synthesis of new compounds permitted the facile preparation of families of related molecules, providing simple (s = 1/2) model systems with which to test emerging theories and propose new experiments.[1] In 1952 Bleaney and Bowers published a study of the magnetic properties of copper(II) acetate monohydrate,[2] and some twenty three years later Hatfield and Hodgson published a magneto-structural correlation (MSC) demonstrating the linear relationship between the strength of the magnetic exchange interaction, J, and the Cu–O–Cu bridging angle in an extended family of bis(μ-hydroxido)copper(II) dimers.[3,4] The first pre-designed construction of a molecule containing ferromagnetically coupled metal ions then followed in 1978 with the molecule [CuVO(fsa)$_2$en] (where (fsa)$_2$en^{4-} is the bi-chelating ligand derived from the Schiff-base bis-(2′-hydroxy-3′-carboxybenzylidene)-1,2-diaminoethane) in which the magnetic orbitals on the constituent metal ions were rigorously orthogonal.[5] The modern era has seen researchers turning their attention to increasingly more complex systems to examine, for example, spin frustration effects in Archimedean and Platonic solids such as Cu^{II} cuboctahedra,[6] and spin-electric coupling in antiferromagnetic [Cu^{II}_3] triangles resulting from the interplay between exchange, spin–orbit coupling and spin chirality.[7]

In the sixty or so years since the initial magnetic study of [$Cu(OAc)_2{\cdot}H_2O]_2$ numerous different ligand types have been employed to construct molecules containing multiple Cu^{II} ions.[8] However, one ligand type which can be almost entirely *excluded* from this list are the phenolic oximes (R-saoH$_2$), since they have been shown to have an overwhelming propensity to form mononuclear complexes of the type [Cu(R-saoH)$_2$] in near quantitative yields.[9] Indeed their remarkable selectivity for copper in the 2+ oxidation state has been exploited in industrial hydrometallurgy, with almost a quarter of the world's copper production involving salicylaldoxime-based ligands.[9] This peculiar selectivity can be ascribed to the tendency of the ligands to form hydrogen bonded head-to-tail dimers mediated *via* intermolecular interactions between the oximic hydrogen atom on one unit and the phenolic oxygen

[a]*EaStCHEM School of Chemistry, The University of Edinburgh, David Brewster Road, Edinburgh, EH9 3FJ, UK. E-mail: ebrechin@staffmail.ed.ac.uk; Tel: +44 (0)131-650-7545*
[b]*Department of Chemistry, Indian Institute of Technology Bombay, Powai, 400076 Mumbai, India. E-mail: rajaraman@chem.iitb.ac.in*

†Electronic supplementary information (ESI) available: Synthetic procedures, crystallographic details, packing diagrams and further details of the DFT calculations. CCDC 991823–991828 and 1029554–1029556. For ESI and crystallographic data in CIF or other electronic format see DOI: 10.1039/c5dt00884k

Open Access Article. Published on 02 April 2015. Downloaded on 4/3/2026 6:59:41 AM.
This article is licensed under a Creative Commons Attribution 3.0 Unported Licence.

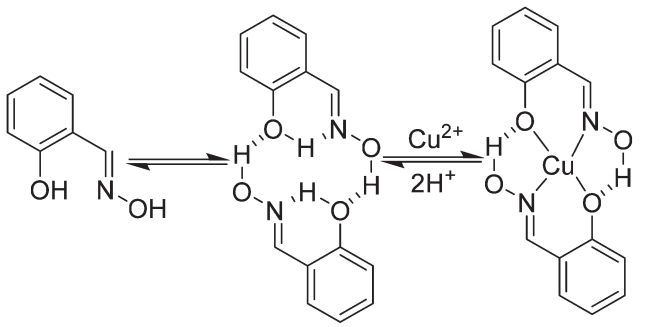

Fig. 1 The pre-organisation of phenolic oximes for the formation of $[Cu^{II}(R\text{-}saoH)_2]$ species.

atom of its neighbour (Fig. 1). The resulting pseudo-macrocyclic cavity facilitates metal complexation, and selectivity for Cu^{II} arises from the goodness-of-fit of this metal cation with the cavity.[10]

Given the above, it is perhaps unsurprising that a search of the CSD reveals that there is only one example of a polymetallic Cu^{II} cage containing two or more metal ions stabilised solely by phenolic oximes.[11] The complex, $[Cu_6(L3\text{-}2H)_3(\mu_3\text{-}O)(\mu_3\text{-}OH)](PF_6)_3$, describes two $[Cu^{II}{}_3O]$ triangles linked by three "double-headed" phenolic oximes, and forms when the ligand : metal ratio employed in the reaction mixture is low; *i.e.* when the metal ions are present in excess.[11] Perhaps the historical observation of a lack of variety in the coordination chemistry of Cu^{II} with phenolic oximes has prevented others from investigating the chemistry further, but the formation of the hexametallic $Cu^{II}{}_6$ species is clear evidence that more interesting structures remain undiscovered. Indeed the $[Cu^{II}{}_3O(oxime)_3]$ triangles of the hexametallic cage are entirely analogous to the building blocks previously observed for Mn^{III}, Fe^{III} and Cr^{III}; all of which present more varied and more interesting structural and physical chemistry.[12] In order to address this "*misperception*" and to prove that polymetallic cages of Cu^{II} can be built with this ligand type, we have adopted a synthetic approach which has already proven successful in Mn chemistry.[13] While both salicylaldoxime and diethanolamine have very limited track records in Cu^{II} chemistry (a CSD search for the latter also returns only monometallic complexes) their combination into one single organic structural framework has the potential to transform the coordination abilities of both. Herein we show that this complimentary ligand approach to constructing novel polymetallic cluster compounds works rather well, by presenting the synthesis, structures and magnetic behaviour of a large and unusual family of Cu^{II}-based wheels constructed using the pro-ligands H_4L_1 and H_4L_2 (Fig. 2).

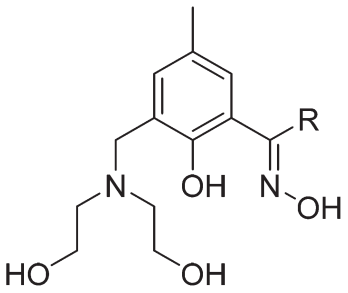

Fig. 2 Generalised molecular structure of the pro-ligands H_4L_1 (R = Me) and H_4L_2 (R = Et).

Experimental

Materials and physical measurements

All manipulations were performed under aerobic conditions using materials as received (reagent grade). The ligand H_4L_1 {1-(3-((bis(2-hydroxyethyl)amino)methyl)-2-hydroxy-5-methyl)phenyl)ethanone oxime} was synthesised according to published procedures.[13a] The synthesis of H_4L_2 {1-(3-((bis(2-hydroxyethyl)amino)methyl)-2-hydroxy-5-methyl)propiophenoneoxime} was achieved by adapting the literature preparation of H_4L_1 (see the ESI† for full details). Variable temperature, solid-state direct current (dc) magnetic susceptibility data down to 5 K were collected on a Quantum Design MPMS-XL SQUID magnetometer equipped with a 7 T dc magnet. Diamagnetic corrections were applied to the observed paramagnetic susceptibilities using Pascal's constants.

Synthesis

$[Cu_8(HL_1)_4(Cl)_4]$ (1). $CuCl_2{\cdot}2H_2O$ (85.24 mg, 0.5 mmol) and H_4L_1 (140 mg, 0.5 mmol) were dissolved in a solvent mixture of MeOH–MeCN (1 : 1, 25 mL). After 5 minutes of stirring, NEt_3 (0.3 mL, 2.1 mmol) was added and the solution stirred for a further 3 h. Large green, block-like X-ray quality crystals were subsequently obtained by slow diffusion of diethyl ether into the filtered mother liquor, over a period of 7 days. Elemental analysis (%) calculated (found) for **1**: C 38.06 (37.98), H 4.57 (4.36), N 6.12 (5.91).

$[Cu_8(HL_1)_4(NO_3)_4]$ (2). $Cu(NO_3)_2{\cdot}3H_2O$ (121 mg, 0.5 mmol) and H_4L_1 (140 mg, 0.5 mmol) were dissolved in a solvent mixture of MeOH–MeCN (1 : 1, 25 mL). After 5 minutes of stirring, NEt_3 (0.3 mL, 2.1 mmol) was added and the solution stirred for a further 3 h. Green, block-like X-ray quality crystals were subsequently obtained by slow diffusion of THF into the filtered mother liquor, over a period of 10 days. Elemental analysis (%) calculated (found) for dried **2**: C 37.13 (36.99), H 4.23 (3.98), N 8.50 (8.41).

$[Cu_8(HL_1)_4(OAc)_4]$ (3). $Cu(OAc)_2{\cdot}H_2O$ (90.54 mg, 0.5 mmol), H_4L_1 (140 mg, 0.5 mmol) were dissolved in a solvent mixture of MeOH–MeCN (1 : 1, 25 mL). After 5 minutes of stirring, NEt_3 (0.3 mL, 2.1 mmol) was added and the solution stirred for a further 3 h. Green, block-like X-ray quality crystals were subsequently obtained by slow diffusion of diethyl ether into the filtered mother liquor, over a period of 7 days. Elemental analysis (%) calculated (found) for dried **3**: C 40.99 (40.87), H 5.38 (4.94), N 5.54 (5.11).

 This journal is © The Royal Society of Chemistry 2015

Open Access Article. Published on 02 April 2015. Downloaded on 4/3/2026 6:59:41 AM.
This article is licensed under a Creative Commons Attribution 3.0 Unported Licence.

$[Cu_8(HL_1)_4(OAc)_2(2,2'\text{-bpy})_2](BF_4)_2$ (4). A mixture of $Cu(BF_4)_2$ (118.6 mg, 0.5 mmol), CH_3COOH (0.30 mg, 0.5 mmol) H_4L_1 (140 mg, 0.5 mmol) and 2,2′-bipyridine (78.09 mg, 0.5 mmol) were dissolved in a solvent mixture of MeOH–MeCN (1 : 1, 25 mL). After 5 minutes of stirring, NEt_3 (0.3 mL, 2.1 mmol) was added and the solution stirred for a further 3 hours. Green, block-like X-ray quality crystals were subsequently obtained by slow diffusion of diethyl ether into the filtered mother liquor, over a period of 7 days. Elemental analysis (%) calculated (found) for dried **4**: C 44.21 (44.16), H 5.32 (5.24), N 6.87 (6.80).

$[Cu_8(HL_1)_4(N_3)_4]$ (5). $Cu(NO_3)_2{\cdot}3H_2O$ (60 mg, 0.25 mmol), H_4L_1 (70 mg, 0.25 mmol) and KN_3 (40 mg, 0.5 mmol) were dissolved in a solvent mixture of MeOH–MeCN (1 : 1, 25 mL). After 5 minutes of stirring NEt_3 (0.15 mL, 1.05 mmol) was added and the solution stirred for a further 3 hours. Large green, block-like X-ray quality crystals were subsequently obtained by slow diffusion of diethyl ether into the filtered mother liquor over a period of 7 days. Elemental analysis (%) calculated (found) for dried **5**: C 37.50 (37.42), H 5.64 (5.33), N 13.05 (12.84).

$[Cu_8(HL_2)_4(Cl)_4]$ (6). $CuCl_2{\cdot}2H_2O$ (85.24 mg, 0.5 mmol) and H_4L_2 (140 mg, 0.5 mmol) were dissolved in a solvent mixture of MeOH–MeCN (1 : 1, 25 mL). After 5 minutes of stirring, NEt_3 (0.3 mL, 2.1 mmol) was added and the solution stirred for a further 3 hours. Large green, block-like X-ray quality crystals were subsequently obtained by slow diffusion of diethyl ether into the filtered mother liquor over a period of 7 days. Elemental analysis (%) calculated (found) for dried **6**: C 41.42 (41.18), H 5.32 (4.81), N 5.68 (5.17).

$[Cu_8(HL_2)_4(Br)_4]$ (7). $CuBr_2{\cdot}2H_2O$ (85.24 mg, 0.5 mmol) and H_4L_2 (140 mg, 0.5 mmol) were dissolved in a solvent mixture of MeOH–MeCN (1 : 1, 25 mL). After 5 minutes of stirring, NEt_3 (0.3 mL, 2.1 mmol) was added and the solution stirred for a further 3 hours. Large green, block-like X-ray quality crystals were subsequently obtained by slow diffusion of diethyl ether into the filtered mother liquor over a period of 7 days. Elemental analysis (%) calculated (found) for dried **7**: C 37.52 (37.42), H 4.72 (4.55), N 5.68 (5.46).

$[Cu_6(HL_1)_4]$ (8). $Cu(OMe)_2$ (60.28 mg, 0.5 mmol) and H_4L_1 (70 mg, 0.25 mmol) were dissolved in a solvent mixture of MeOH–MeCN (1 : 1, 25 mL). After 5 minutes of stirring NEt_3 (0.30 ml, 2.1 mmol) was added and the solution stirred for a further 3 h. Green, block-like X-ray quality crystals were subsequently obtained by slow diffusion of diethyl ether into the filtered mother liquor over a period of 7 days. Elemental analysis (%) calculated (found) for dried **8**: C 44.89 (44.57), H 5.11 (4.88), N 7.48 (7.24).

$[Cu_4Na_2(HL_1)_2(H_2L_1)_2]$ (9). $Cu(BF_4)_2{\cdot}3H_2O$ (118.6 mg, 0.5 mmol) and H_4L (140 mg, 0.50 mmol) were dissolved in a solvent mixture of MeOH–MeCN (1 : 1, 25 mL). After 5 minutes of stirring NaOMe (216 mg, 2 mmol) was added and the solution stirred for a further 3 hours. Green, block-like X-ray quality crystals were subsequently obtained by slow diffusion of hexane into the filtered mother liquor over a period of 12 days. Elemental analysis (%) calculated (found) for dried **9**: C 47.03 (46.91), H 5.71 (5.52), N 7.56 (7.22).

X-ray crystallography

Single crystal X-ray diffraction data of **1–9** were collected at 100 K on a Agilent Technologies SuperNova at temperatures between 200 and 120 K. See Table S1† and CIF files for full details. CCDC 991823–991828 and CCDC 1029554–1029556.

Results and discussion

Complexes **1–7** (Fig. 3–5) share the same general structural framework, and so for the sake of brevity we describe **1** in detail and highlight any significant structural differences present in **2–7**.

The metallic skeleton of complex **1** (Fig. 3) describes a saddle-like or basket shaped, single-stranded, octametallic wheel of approximate radius 7.3 Å, in which all eight Cu^{II} ions are symmetry inequivalent. The coordination geometries of the Cu ions alternate between square planar (Cu1, Cu3, Cu5, Cu7) and square-based pyramidal (Cu2, Cu4, Cu6, Cu8, τ = 0.0743–0.0131) as the wheel is circumnavigated. The HL_1^{3-} ligands each bridge a total of four Cu ions: the oximic and phenolic moieties are μ-bridging (Cu–N–O–Cu, ~19–25°;

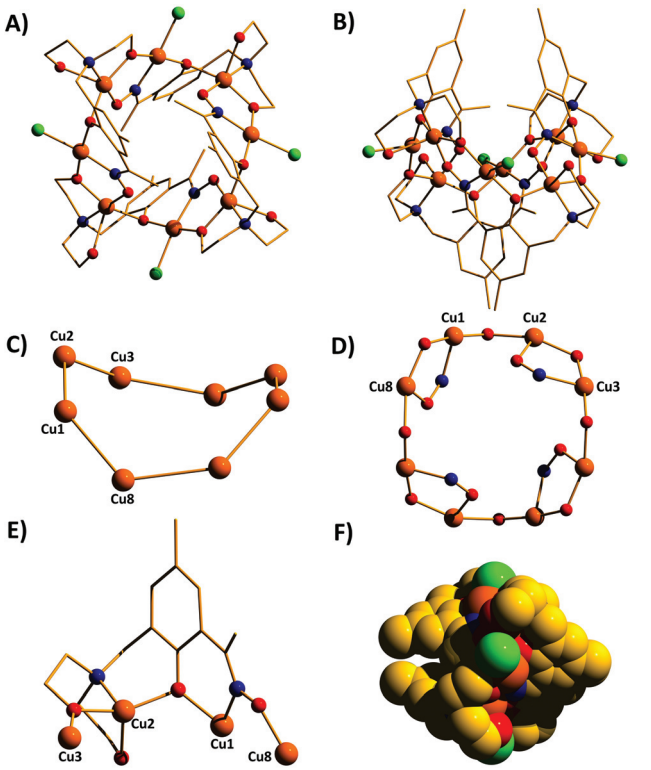

Fig. 3 The molecular structure of complex **1** viewed perpendicular (A) and parallel (B) to the Cu_8 "plane". Colour code, Cu = orange, O = red, N = blue, C = gold, Cl = green. (C) The metallic skeleton of **1** highlighting the bowl-shape of the cluster. (D) The magnetic core of **1** showing the two different exchange interactions. (E) The bridging mode of the HL_1^{3-} ligand. (F) Space-fill representation of **1**. H atoms omitted for clarity.

Open Access Article. Published on 02 April 2015. Downloaded on 4/3/2026 6:59:41 AM.
This article is licensed under a Creative Commons Attribution 3.0 Unported Licence.

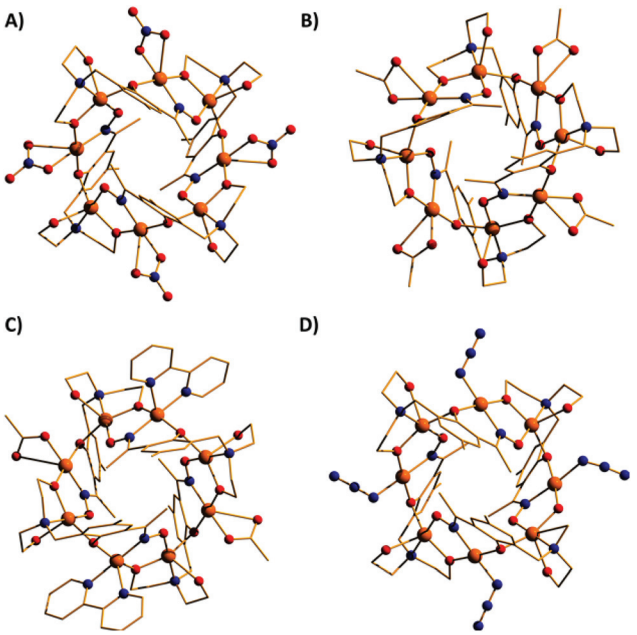

Fig. 4 The molecular structures of complexes **2–5** (A–D). Colour code as Fig. 3.

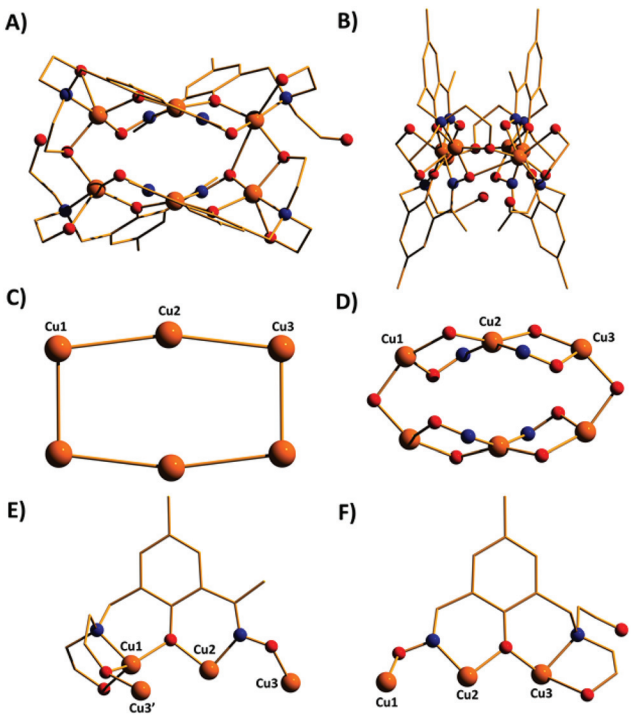

Fig. 5 The molecular structure of complex **8** viewed perpendicular (A) and parallel (B) to the Cu_6 plane. Colour code, Cu = orange, O = red, N = blue, C = gold. (C) The metallic skeleton of **8** highlighting the bowl-shape of the cluster. (D) The magnetic core of **8** showing the two different exchange interactions. (E/F) The two bridging modes of the HL_1^{3-} ligand. H atoms omitted for clarity.

Cu–O–Cu, ~16°), with one alkoxide arm of the diethanolamine moiety μ-bridging (Cu–O–Cu, ~18°) and the other remaining protonated and terminally bonded (Cu–O, 2.317–2.433 Å). The remaining coordination sites on the square planar Cu ions are occupied by Cl^- anions, which are H-bonded to the terminally bonded O-atoms of the diethanolamine arms (Cl···O, ~3 Å). Each Cu ion is therefore linked to its neighbours by one alkoxide and one oximic –N–O– moiety on one side, and by just one phenoxide on the other. The magnetic core is thus rather simple: $[Cu–OR/NO–Cu–OR]_4$. Two of the HL_1^{3-} ligands point above and two point below the plane of the bowl, each orientated inwards toward the centre of the bowl resulting in a (C···C) separation of ~3.5 Å. The closest intermolecular contacts are between the Cl^- ions and the *para*-Me(Ph) groups of the HL_1^{3-} ligands at a (Cl···C) distance of ~3.7 Å. The result is that molecules of **1** pack in a serpentine-like manner when viewed down the *b*-axis (Fig. S2 in the ESI†).

The molecular structures of complexes **2–5** are shown in Fig. 4. Structural differences between **1** and **2–5**, bar changes in the crystallographic/symmetry parameters (Table S1 in the ESI†) and small changes in the bond lengths and angles, are limited to the terminally bonded Cl^- ions being been replaced by chelating NO_3^- ions in **2**, chelating $CH_3CO_2^-$ ions in **3** and terminally bonded N_3^- ions in **5**. In complex **4** two of the Cl^- ions have been replaced by chelating $CH_3CO_2^-$ ions and two by chelating 2,2′-bpy molecules, with charge balance maintained through the presence of two BF_4^- counter anions. The chelating ligands change the geometry of the Cu^{II} ions at these sites to distorted trigonal bipyramidal, meaning that the wheels **2–4** contain eight trigonal bipyramidal metal centres, with only complex **5** maintaining the four coordinate-five coordinate pattern seen in **1**.

The introduction of an Et-group (H_4L_2) as opposed to a Me-group (H_4L_1) at the oximic carbon atom of the ligand appears to exert little structural effect, with complexes **6** and **7** being largely analogous to **1**, with minor changes in bond lengths and bond angles. Complexes **1–7** all contain terminally bonded or chelating anions, introduced to the reaction mixture in the copper salt. In order to examine the effect of removing this anion, we repeated the synthesis employing the methoxide salt of Cu^{II}. The reaction between anhydrous $Cu(OMe)_2$ and H_4L_1 in a basic MeOH–MeCN solution afforded the homoleptic, hexametallic wheel $[Cu_6(HL_1)_4]$ (**8**; Fig. 5). The metallic skeleton of **8** describes a single-stranded hexametallic, rectangular Cu^{II} wheel. The asymmetric unit contains half the wheel, *i.e.* three Cu ions (Cu1–3) and two HL_1^{3-} ligands. The latter are triply deprotonated as before, but coordinate differently in **8** than in **1–7**. One ligand bridges a total of four and the other a total of three metal centres with the oximic and phenolic moieties μ-bridging (Cu–N–O–Cu, ~37°, ~48°; Cu–O–Cu; ~108°, ~113°) in both cases, as in **1–7**. It is the alkoxide arms of the diethanolamine moiety of the two symmetry inequivalent ligands which behave differently: in one ligand, one arm is μ-bridging (Cu–O–Cu, 102.5°) with the other terminally bonded at the apical site of the Cu square-based pyramid (Cu–O, 2.35 Å); in the second, one arm is terminally bonded (Cu–O,

 This journal is © The Royal Society of Chemistry 2015

Open Access Article. Published on 02 April 2015. Downloaded on 4/3/2026 6:59:41 AM.
This article is licensed under a Creative Commons Attribution 3.0 Unported Licence.

2.4 Å) and one non-bonded, and H-bonding to the bridging alkoxide from a neighbouring HL^{3-} ligand (O···O, ~2.6 Å). The coordination geometries of the Cu ions are thus mixed: Cu2 is four coordinate and square planar, whilst Cu1 and Cu3 are five coordinate and square-based pyramidal (τ = 0.118 and 0.0775 respectively). The metallic skeleton is near planar, as opposed to the puckered structures of **1–7**, with the short and long edges of the rectangle measuring ~3 Å and ~6 Å, respectively. As before, one pair of HL_1^{3-} ligands points above and one pair below the plane of the wheel, with the aromatic rings being separated by approximately 3.5 Å. The closest intermolecular interactions occur between the *para*-Me(Ph) groups of the ligand on one molecule and the terminally bonded O atom of the diethanolamine arms on its neighbour (~3.7 Å, Fig. S3†).

A repetition of the reaction that produces complex **8**, but using $Cu(BF_4)_2{\cdot}3H_2O$ in place of anhydrous $Cu(OMe)_2$ and employing NaOMe instead of NEt_3 results in the formation of $[Cu_4Na_2(HL_1)_2(H_2L_1)_2]$ (**9**; Fig. 6). The metallic skeleton of complex **9** also describes a hexametallic wheel, but on this occasion it is heterometallic, more hexagonal than rectangular, and non-planar. The asymmetric unit includes the Cu_2Na trimeric moiety, (Cu1–Na1, ~6.4 Å; Cu1–Na1′, ~3.2 Å) with the Na...Na diameter of the wheel being ~6.9 Å, and the closest Cu...Cu distance ~4.9 Å (Cu2...Cu2′). Cu1 is five coordinate and trigonal bipyramidal (τ = 0.14), whilst Cu2 is four-coordinate and square planar in geometry. The ligands are of two types: HL_1^{3-} and $H_2L_1^{2-}$ (Fig. 6E and 6F). The former bridges a total of four metal centres, with the oximic and phenolic moieties μ-bridging (Cu–N–O–Cu; ~50°; Cu–O–Cu, ~112°), one alkoxide arm of the diethylamine moiety is μ-bridging between Cu1 and Na1′, with the second arm terminally bonded to Cu1 and H-bonded to a neighbouring oximic O-atom (~2.6 Å). The second ligand uses its oximic O-atom (O6) to bridge between Cu1 and Na1; its oximic N-atom also bonded to Cu1. The phenoxide O-atom μ-bridges between Cu2 and Na1, with both diethanolamine arms being terminally bonded to Na1. The Na^+ ions are six-coordinate and in distorted octahedral geometries. There are two intramolecular H-bonding interactions per molecule; between the H-atom of the protonated diol arm of one ligand and the oximic O-atom of its symmetry equivalent (O···H = ~2.6 Å°). The closest intercluster contacts are between the coordinated O-atom of one diethanolamine arm and the CH_2 groups of a neighbouring arm (~3.2 Å; Fig. S4 and S5 in the ESI†). Complex **9** is clearly rather similar in structure to complex **8**, the major difference being the introduction of the larger Na^+ ions in the former. This has the effect of severely twisting of the M–M–M trimer of the asymmetric unit, from ∠Cu–Cu–Cu = 166° for **8** to ∠Cu–Cu–Na = ~146° in **9**. This has two consequences for the latter complex: firstly the metallic skeleton becomes more bowl-shaped, and secondly there are no longer any coplanar ligands lying perpendicular to the M_6 mean plane. Indeed the *para*-Me(Ph) moieties now point outward rather than inward as seen in all the previous cages (compare Fig. 5B and 6B).

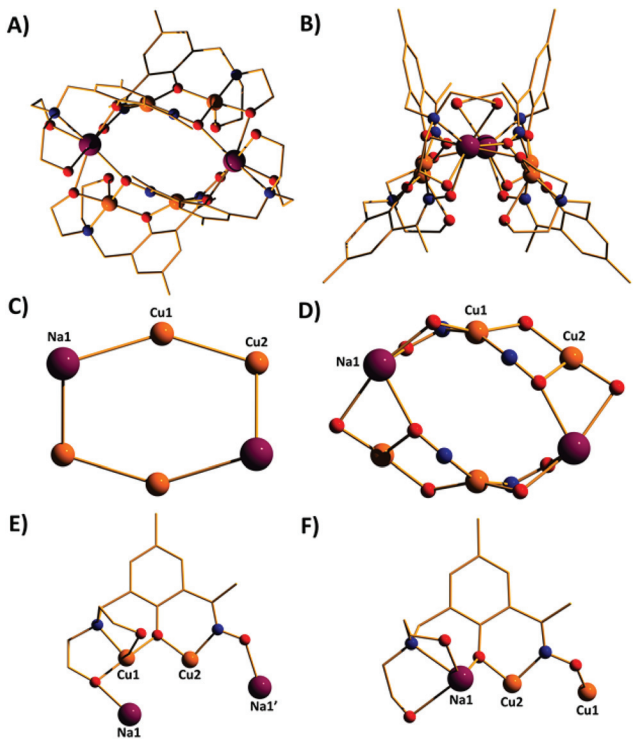

Fig. 6 The molecular structure of complex **9** viewed perpendicular (A) and parallel (B) to the Cu_4Na_2 "plane". Colour code, Cu = orange, Na = purple, O = red, N = blue, C = gold. (C) The metallic skeleton of 9 highlighting the bowl-shape of the cluster. (D) The magnetic core of 9 showing the two different exchange interactions. (E) The bridging mode of the H_1L^{3-} ligand (F) The bridging mode of the H_1L^{3-} ligand. H atoms omitted for clarity.

It is difficult at this stage to definitively correlate the changes in syntheses, as summarised in Fig. 7, to the observed structural changes. The simplest reaction is that between $Cu(OMe)_2$ and H_4L_1, which produces $[Cu_6(HL)_4]$ (**8**) and MeOH. The same product results from reactions employing different alkoxide precursors. Thus it seems the alcohol produced does not bond to the Cu^{II} ions. When the anion of the metal salt is changed to one that is commonly found to chelate, bond terminally or even bridge between metal centres, or if that anion is added separately to the reaction mixture (halide, pseudohalide, carboxylate), the nuclearity of the cage increases to $[Cu_8]$ despite the fact that this anion is non-bridging. Much of this seems rather counter-intuitive at first: one might expect the removal of terminally bonded anions to promote increased bridging of HL_1^{3-} and/or to encourage further deprotonation to L_1^{4-}. However this does not occur, and even the addition of an excess of base does not achieve this transformation. We can only surmise that the addition of a bonding anion forces a change in the metal geometry which in turn forces a change in the bonding mode of the ligand and thus to different cluster nuclearities and topologies. The introduction of the alkali metal ion Na^+, in the form of NaOMe, suggests other heterometallic cages can be made by simply employing alternative group 1 or group 2 alkoxides, although we have not investigated this further.

Open Access Article. Published on 02 April 2015. Downloaded on 4/3/2026 6:59:41 AM.
This article is licensed under a Creative Commons Attribution 3.0 Unported Licence.

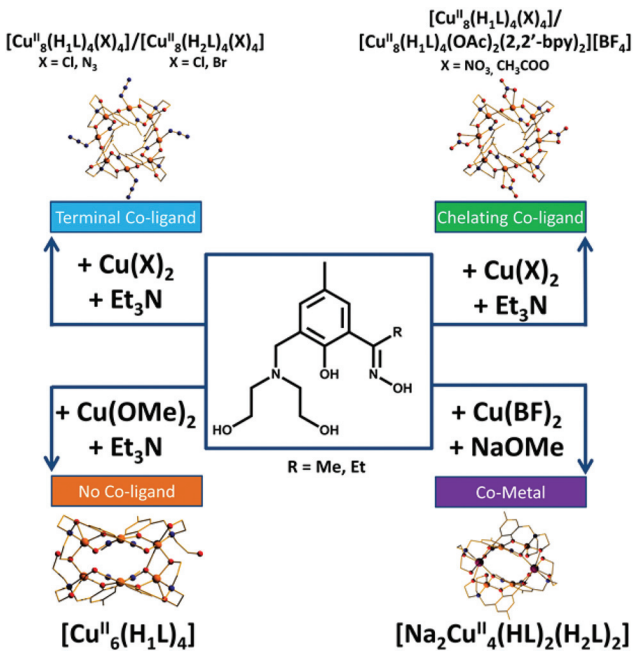

Fig. 7 Summarising the effect changes in CuX_2 starting material has on product formation with $H_4L_{1/2}$.

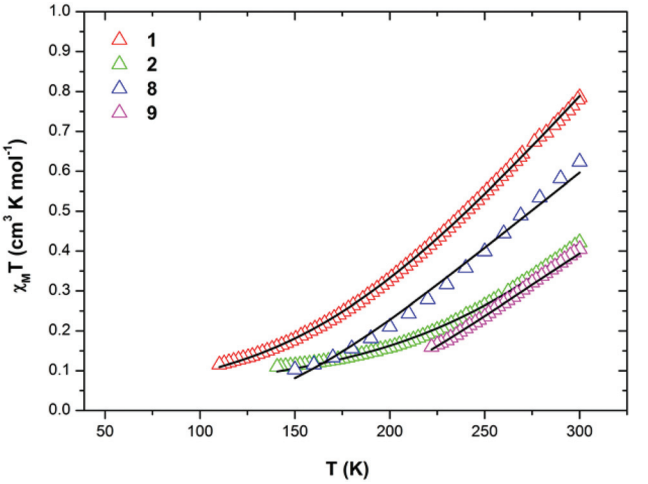

Fig. 8 The magnetic susceptibility data, as $\chi_M T$, *versus* T at B = 0.1 T for complexes **1** (red), **2** (green), **8** (blue) and **9** (magenta). The solid black lines are fits of the experimental data. The best fit 3J model is shown for **8**. See text for details.

A search of the CSD reveals that there are thirteen examples of O-bridged, single-stranded homo-metallic Cu^{II} wheels of nuclearity ≤ 8 in the literature. Of these, seven are octametallic[14–20] and six are hexametallic.[21–26] There are many more examples of both octametallic and hexametallic single-stranded Cu wheels which contain bridging motifs that do not feature oxygen atoms.[27] To the best of our knowledge there are no reported examples of single-stranded heterometallic wheels of nuclearity six with a Cu : M (where M is an alkali metal cation) ratio of 4 : 2. Complexes **1–7** therefore become only the 12th examples of O-bridged single-stranded octametallic Cu^{II} wheels, complex **8** only the 7th example of a single-stranded hexametallic Cu^{II} wheel, and complex **9** the first example of a single-stranded heterometallic Na/Cu^{II} wheel. Apart from their rather beautiful structural aesthetics, molecular wheels have long held fascination for both chemists and physicists, since they can often act as model compounds for the study of quantum effects and spin frustration.[28] and have recently been identified as potential candidates for quantum information processing.[29]

Magnetochemistry

DC magnetic susceptibility. Dc magnetic susceptibility measurements were collected for complexes **1**, **2**, **8** and **9**, in the T = 300–5 K temperature range in an applied field of B = 0.1 T. The data are plotted in Fig. 8 as the $\chi_M T$ *versus* T products. Complexes **1** and **2** are representative examples of the two structurally different Cu_8 wheels, with **8** and **9** being the Cu_6 and Cu_4Na_2 wheels, respectively. The data for all four complexes are rather similar – showing a rapid decrease in $\chi_M T$ with decreasing temperature, indicative of the presence of very strong antiferromagnetic interactions between neighbouring Cu^{II} ions, resulting in diamagnetic ground states (at T = 110–220 K) in all cases. We have used the programme ITO-MAGFIT[30] which makes use of irreducible tensor operator algebra[31] to block-diagonalise the spin-Hamiltonian in order to model the experimental data. In all cases the g-values of the Cu(II) ions were fixed to g = 2.2. The resulting best-fit curves obtained in this way are shown as solid black lines in Fig. 8 with the corresponding best-fit parameters listed in Table 1. A schematic of the models employed is shown in Fig. 9. For the Cu_8 clusters best-fit J-values reveal that the exchange through the Cu–O/NO–Cu bridge is very large and negative (J_1 = −457 and −302 cm^{-1} for **1** and **2** respectively), with the exchange through the Cu–O–Cu bridge also antiferromagnetic but smaller in magnitude (J_2 = −20.1 and −38.9 cm^{-1} for **1** and **2** respectively). The differences can be correlated to subtle differ-

Table 1 Comparison of J values obtained from the fitting of experimental data to the models depicted in Fig. 9, and those from DFT calculations

Complex/method	J_1 (cm^{-1})	J_2 (cm^{-1})	J_3 (cm^{-1})	J_4 (cm^{-1})
1/Fit	−20.1	−457	—	—
1/DFT	−45.0	−320	—	—
2/Fit	−38.9	−302	—	—
2/DFT	−46.6	−278	—	—
8/Fit (2J)	−200	−247	−247	—
8/Fit (3J)	−107	−239	−260	—
8/DFT	+5.50	−25.9	−120	—
9/Fit	—	−271	—	—
9/DFT	—	−95.8	—	+0.08

This journal is © The Royal Society of Chemistry 2015

Open Access Article. Published on 02 April 2015. Downloaded on 4/3/2026 6:59:41 AM.
This article is licensed under a Creative Commons Attribution 3.0 Unported Licence.

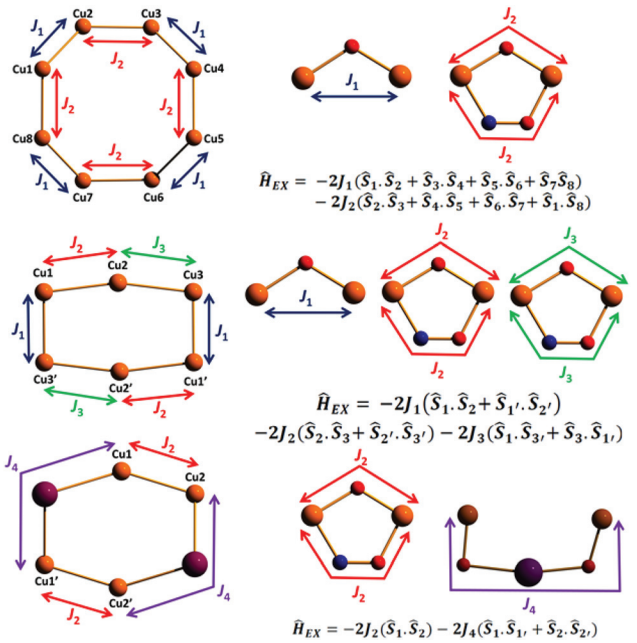

Fig. 9 The magnetic cores of the representative Cu_8, Cu_6 and Cu_4Na_2 metal cores (left) and the models representing the exchange component of the spin-Hamiltonians which their experimental susceptibility data were fitted to (right). For the experimental fit of **9** $J_4 = 0$.

ences in structure: a) the Cu–O–N–Cu dihedral angles are flatter in **1** (~19, 20, 21, 25°) than in **2** (~23, 23, 24, 24°); b) the Cu–O–Cu angles in **1** are typically larger than **2** (~115–118° *versus* ~110–118°). The former would be expected to make J_2 larger in **1**, and the latter make J_1 larger in **2**, as observed. For complex **8**, the best fit of the experimental data is afforded by a 3*J* model, accounting for the single alkoxide bridge (J_1) and the two NO/O bridges which display markedly different bridging angles (48.17, 37.47; J_2 and J_3). The best fit parameters obtained were $J_1 = -107$, $J_2 = -239$ and $J_3 = -260$ cm^{-1}. This fit however is not unique and we were able to obtain several satisfactory fits using a 2*J* model (see Table 1). Nevertheless, the parameters of the 3*J* best fit are consistent with those obtained for **1** and **2** in which J(O/NO) > J(O) and with the larger torsion angle mediating weaker antiferromagnetic exchange. Complex **9** describes a wheel comprising two simple, non-interacting Cu(II) dimers in which we assume negligible interaction through the Cu–Na–Cu bridge. This model affords a best fit $J_2 = -271$ cm^{-1}. The exchange is again antiferromagnetic in nature, but somewhat larger than observed for **1**, **2** and **8**. A literature search reveals only three examples of dimers which feature Cu–O/NO–Cu moieties, but on which no magnetic studies have been reported.[32] There are several examples of polymetallic Cu systems featuring Cu–O/NO–Cu bridging motifs,[33] and all show the interaction to be strongly antiferromagnetic. The magnitude of the exchange interaction in purely alkoxo-bridged Cu(II) dimers varies enormously and is dependent on the Cu–O–Cu angle, but in general they tend to be strongly antiferromagnetic with J lying in the region −200 to −1000 cm^{-1}.[34] A similar pattern is seen in purely oximato bridged Cu(II) dimers, where J ranges from −361 cm^{-1} to −880 cm^{-1},[35] although in the vast majority of cases J appears to lie in the region −600 to −800 cm^{-1}. In order to investigate the origin and magnitude of the exchange interactions seen in complexes **1**, **2**, **8** and **9** further we have turned to theory, and now discuss a computational DFT study.

Theoretical studies

Computational details. Calculations were performed using the B3LYP[36] functional, with Alhrich's triple-ζ TZV[37] basis set for the Cu(II) ions and SV basis sets for the remaining atoms, as implemented in the Gaussian 09[38] suite of programs. The exchange constants between the Cu(II) ions were calculated as the energy difference between the high spin state (E_{HS}) using single determinant wave functions, and the low spin state (E_{BS}) using Noodleman's broken symmetry approach.[39–42] The exchange Hamiltonians adopted are the same as those described in the experimental section above (Fig. 9). In complex **1** there are two unique exchange interactions denoted as J_1 and J_2, mediated *via* a μ-phenoxo bridge and a μ-alkoxo/oxime bridge, respectively. Calculations yield $J_1 = -45.0$ cm^{-1} and $J_2 = -320$ cm^{-1}. Both interactions are computed to be antiferromagnetic in nature with J_2 being very strong. To cross check, calculations were also performed using a diamagnetic substitution method whereby all metal centres not involved in the exchange interaction were replaced with diamagnetic Zn(II) ions. This method yielded a very similar set of J values, $J_1 = -35.1$ cm^{-1} and $J_2 = -300$ cm^{-1}. Fitting of the experimental susceptibility data also yields similar J values, indicating weak antiferromagnetic J_1 and strong antiferromagnetic J_2 interactions (see Table 1), as would be expected since their Cu–O–Cu angles are rather similar (115.8°, 118.6°). However their magnitude is much smaller than might be anticipated from previous magnetostructural correlations.[43] This results from the puckering of the ring: the unpaired electron in Cu(II) is found in the $d_{x^2-y^2}$ orbital and the buckled nature of the wheel results in the two magnetic orbitals (corresponding to the J_1 interaction) being in different planes (Fig. S6†), weakening the interaction. This is in stark contrast to the J_2 interactions where the oxime moiety forces the $d_{x^2-y^2}$ orbitals to be in same plane, leading to a very strong interaction. The magnitude of exchange in Cu(II) complexes can be correlated directly to the energy gap between the symmetric and antisymmetric combinations of the $d_{x^2-y^2}$ orbitals. The oxime bridge present in J_2 produces a complementarity effect whereby the π* orbitals of the oxime interacts with the antisymmetric combination (Fig. 10), leading to a larger energy gap and hence to stronger antiferromagnetic coupling.

The overlap integrals, computed as 0.08 and 0.20 for J_1 and J_2, respectively, confirm this. Computed spin density plots for complexes **1**, **8**, and **9** are shown in Fig. 11. The Cu(II) centres in complex **1** possess spin densities of 0.63 [Cu(1)] and 0.59 [Cu(2)], values substantially lower than the expected value of 1.0, revealing significant delocalisation (and hence strong exchange) of the unpaired spin onto the bridging ligands. The

Open Access Article. Published on 02 April 2015. Downloaded on 4/3/2026 6:59:41 AM.
This article is licensed under a Creative Commons Attribution 3.0 Unported Licence.

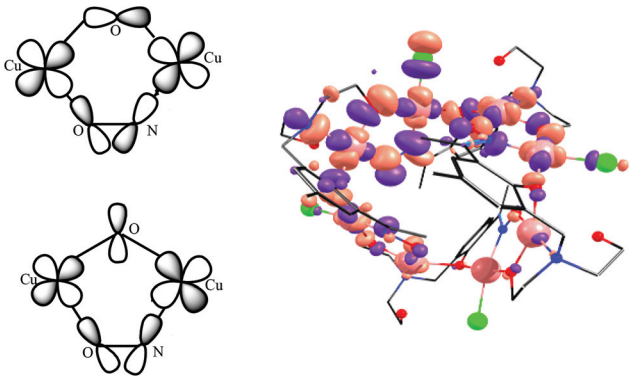

Fig. 10 Schematic representation of the complementarity effect exhibited by the oxime bridge with symmetric and antisymmetric combinations of $d_{x^2-y^2}$ orbitals (left) and a representative MO diagram depicting the antisymmetric combination of the $d_{x^2-y^2}$ orbitals (right).

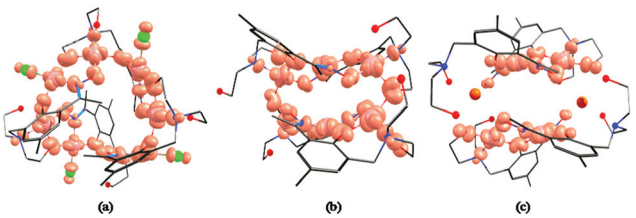

Fig. 11 B3LYP computed spin density plots of complex **1** (a), **8** (b) and **9** (c).

spin density on the bridging groups are also significant, 0.12 on the O-atom of the μ-alkoxide (J_1), and 0.16 on the O-atom of the μ-alkoxide, and 0.13 and 0.10 for O and N atoms of the oxime bridge in the J_2 interaction.

For complex **2** calculations yield a similar set of exchange constants, although the J_2 interaction is computed to be slightly smaller (Table 1). The decrease in the magnitude of the J_2 interaction compared to complex **1** is found to correlate to the Cu–O–N–Cu dihedral angle. In complex **2** the bulkier, chelating nitrate groups cause a twist in the Cu–N–O–Cu dihedral leading to weaker $d_{x^2-y^2} - d_{x^2-y^2}$ overlap and a reduction in the J values. The spin density on the Cu(II) centres in complex **2** are plotted in Fig. S7.†

For complex **8** calculations yield J_1 = +5.53 cm^{-1}, J_2 = −25.9 cm^{-1} and J_3 = −120 cm^{-1}. The J_1 interaction is computed to be weakly ferromagnetic in nature, in contrast to that fitted experimentally. Here the Cu–O–Cu angle is relatively small (102.2°) and along with the large out-of-plane shift of the O–C(alkyl) group from the Cu–O–Cu–O plane (~40.0°) the geometry is approaching that theoretically predicted to mediate ferromagnetic exchange;[44] the crossover area likely being the source of error in the theoretical calculation. J_2 and J_3 are antiferromagnetic in nature with J_3 being approximately five times larger. This is again correlated to the difference in the Cu–N–O–Cu dihedral angle, with smaller angles yielding stronger antiferromagnetic coupling. The magnitude of the J_2 and J_3 interactions are much smaller than that computed for complexes **1** and **2** due to the smaller ring size – the Cu–N–O–Cu moieties being far more twisted than that found in complexes **1** and **2**. For complex **9** the computed exchange constants are J_2 = −95.8 cm^{-1} and J_4 = +0.08 cm^{-1}. The former is consistent with that observed in previous complexes, and the latter as expected for an interaction mediated through a diamagnetic Na^+ ion. Computed overlap integrals (0.26 and 0.005 for J_2 and J_4, respectively) are consistent with this picture (Fig. S8†). In all four complexes the strongest antiferromagnetic coupling constant is underestimated by DFT, the differences being particularly obvious when the other J values are small in magnitude. The underestimation of the exchange interactions in Cu(II) complexes by DFT has been highlighted previously,[45] and is thus a limiting factor in the accurate estimation of absolute values.

Since the Cu–N–O–Cu dihedral has been found to play an important role in determining the J values in this family of complexes, we have developed a magneto-structural correlation based on a dimeric model of complex **9** shown in the inset of Fig. 12. By varying the Cu–N–O–Cu dihedral angle (x) [with the Cu–O–Cu angle fixed] from 0–80° an exponential correlation was found, with the smallest dihedral angles leading to the strongest AF exchange, and the largest dihedral angles leading to the weakest AF exchange. Fitting the data to the expression

$$-J = Ae\left[\frac{x}{t}\right] + y_o$$

yields y_o = −608, A = 262, t = −79.5, revealing a switch from AF to F exchange at dihedral angles >60°. Attempts are underway to isolate wheels with this large degree of puckering in order to test this theory.

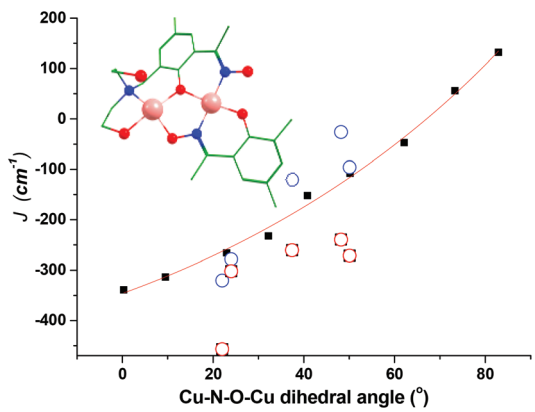

Fig. 12 Magnetostructural correlation developed by DFT calculations by varying the Cu–N–O–Cu dihedral angle in a model complex based on complex **9**. The solid black squares are computed points and the red line the best fit to these points. The hollow blue circles are the DFT calculated values for the full structure, whilst the red circles are the experimentally fitted exchange constants.

This journal is © The Royal Society of Chemistry 2015

Open Access Article. Published on 02 April 2015. Downloaded on 4/3/2026 6:59:41 AM.
This article is licensed under a Creative Commons Attribution 3.0 Unported Licence.

Conclusions

The simple reaction of Cu(II) salts with diethanolamine-functionalised phenolic oximes has resulted in seven new examples of single-stranded octametallic Cu(II) wheels, one new example of a single-stranded hexametallic Cu(II) wheel, and the first reported example of a single-stranded hexametallic mixed-metal Na_2Cu_4 wheel. The construction of polymetallic cages from ligand moieties normally associated with producing monometallic Cu(II) compounds is clear evidence that combining complimentary ligand types into one organic framework is a sensible methodology for building polymetallic cluster compounds. In each case the interaction between neighbouring metal ions was shown to be strongly antiferromagnetic. DFT calculations suggest the origin to be a complementarity effect due to the presence of the oxime bridge, in which smaller Cu–N–O–Cu dihedral angles yield larger exchange constants, which are inherently linked to the planarity of the wheel. A magnetostructural correlation developed even suggests that such Cu(II) wheels can be made to display intramolecular ferromagnetic exchange if the Cu–N–O–Cu torsion angles can be of the order of 60° or larger. Current efforts are aimed at synthetic strategies to achieve just that.

Acknowledgements

The authors acknowledge the EPSRC (UK). GR would like to thank the AISRF and DST Nanomission (SR/NM/NS-1119/2011) for funding. NV would like to thank the DST for a fast track fellowship.

Notes and references

1 D. Gatteschi, O. Kahn and R. D. Willett, *Magnetostructural Correlations in Exchange Coupled Systems*, D. Reidel, Dordrecht, 1985.
2 B. Bleaney and K. D. Bowers, *Proc. R. Soc. London, Ser. A*, 1952, **214**, 451.
3 V. H. Crawford, H. W. Richardson, J. R. Wasson, D. J. Hodgson and W. E. Hatfield, *Inorg. Chem.*, 1976, **15**, 2107.
4 W. E. Hatfield, *Comments Inorg. Chem.*, 1981, **1**, 105.
5 O. Kahn, J. Galy, P. Tola and H. Coudanne, *J. Am. Chem. Soc.*, 1978, **100**, 3931.
6 A. Honecker and M. E. Zhitomirsky, *JCPS*, 2009, **145**, 012082.
7 M. Triff, F. Troiani and D. Loss, *Phys. Rev. Lett.*, 2008, **101**, 217201.
8 See for example: (*a*) C. P. Landee and R. E. Greenery, *Inorg. Chem.*, 1986, **25**, 3771; (*b*) G. D. Fallon and K. S. Murray, *Inorg. Chim. Acta*, 1985, **96**, L53; (*c*) H. Uekusa, S. Ohba, T. Tokii, Y. Muto, M. Kato, S. Husbye, O. W. Steward, S. Chang, J. P. Rose, J. F. Pletcher and I. Suzuki, *Acta Crystallogr., Sect. B: Struct. Sci.*, 1992, **48**, 650; (*d*) R. Costa, P. R. Moreira, S. Youngme, K. Siriwong, N. Wannarit and F. Illlas, *Inorg. Chem.*, 2010, **49**, 285; (*e*) T. Yamase, H. Ishikawa, H. Abe, K. Fukaya, H. Nojiri and H. Takeuchi, *Inorg. Chem.*, 2012, **51**, 4606.
9 P. A. Tasker, P. G. Plieger and L. C. West, *Compr. Coord. Chem. II*, 2004, **9**, 759.
10 A. G. Smith, P. A. Tasker and D. J. White, *Coord. Chem. Rev.*, 2003, **241**, 61.
11 M. Wenzel, R. S. Forgan, A. Faure, K. Mason, P. A. Tasker, S. Piligkos, E. K. Brechin and P. G. Plieger, *Eur. J. Inorg. Chem.*, 2009, 4613.
12 See for example: (*a*) R. Inglis, C. J. Milios, L. F. Jones, S. Piligkos and E. K. Brechin, *Chem. Commun.*, 2012, **48**, 181; (*b*) K. Mason, I. A. Gass, F. J. White, G. S. Papaefstathiou, E. K. Brechin and P. A. Tasker, *Dalton Trans.*, 2011, **40**, 2875; (*c*) P. Chaudhuri, M. Hess, E. Reutschler, T. Weyhermuller and U. Florke, *New J. Chem.*, 1998, 553.
13 See for example: (*a*) S. Sanz, J. M. Frost, T. Rajeshkumar, S. J. Dalgarno, G. Rajaraman, W. Wernsdorfer, J. Schnack, P. J. Lusby and E. K. Brechin, *Chem. – Eur. J.*, 2014, **20**, 3010; (*b*) S. Sanz, J. M. Frost, M. B. Pitak, S. J. Coles, S. Piligkos, P. J. Lusby and E. K. Brechin, *Chem. Commun.*, 2014, **50**, 3310; (*c*) J. M. Frost, S. Sanz, T. Rajeshkumar, M. B. Pitak, S. J. Coles, G. Rajaraman, W. Wernsdorfer, J. Schnack, P. J. Lusby and E. K. Brechin, *Dalton Trans.*, 2014, **43**, 10690.
14 G. Mezei, P. Baran and R. G. Raptis, *Angew. Chem., Int. Ed.*, 2004, **43**, 574.
15 R. Acevedo-Chavez, M. E. Costas and R. Escudero, *J. Solid State Chem.*, 1997, **132**, 24.
16 (*a*) D. A. Fowler, A. V. Mossine, C. M. Beavers, S. J. Teat, S. J. Dalgarno and J. L. Atwood, *J. Am. Chem. Soc.*, 2011, **133**, 11069; (*b*) H. Kumari, A. V. Mossine, S. R. Kline, C. L. Dennis, D. A. Fowler, S. J. Teat, C. L. Barnes, C. A. Deakyne and J. L. Atwood, *Angew. Chem., Int. Ed.*, 2012, **51**, 1452.
17 G. A. Ardizzoia, M. A. Angaroni, G. La Monica, F. Cariati, M. Moret and N. Masciocch, *J. Chem. Soc., Chem. Commun.*, 1991, 1021.
18 A. Mukherjee, I. Rudra, M. Nethaji, S. Ramasesha and A. R. Chakravarty, *Inorg. Chem.*, 2004, **42**, 463.
19 L. Zherlitsyna, N. Auner and M. Bolte, *Acta Crystallogr., Sect. C: Cryst. Struct. Commun.*, 2006, **62**, 199.
20 H. Kumari, A. V. Mossine, S. R. Kline, C. L. Dennis, D. A. Fowler, S. J. Teat, C. L. Barnes, C. A. Deakyne and J. L. Atwood, *Angew. Chem., Int. Ed.*, 2012, **51**, 1452.
21 M. A. Castro, M. Rusjan, D. Vega, O. Pena, T. Weyhermuller, F. D. Cukiernik and L. D. Slep, *Inorg. Chim. Acta*, 2011, **379**, 499.
22 S. D. Bunge, J. A. Ocana, T. L. Cleland and J. L. Steele, *Inorg. Chem.*, 2009, **48**, 4619.
23 A. A. Mohamed, S. Ricci, A. Burini, R. Galassi, C. Santini, G. M. Chiarella, D. Y. Melgarejo and J. P. Fackler Jr., *Inorg. Chem.*, 2011, **50**, 1014.
24 L. F. Jones, C. A. Kilner, M. P. de Miranda, J. Wolowska and M. A. Halcrow, *Angew. Chem., Int. Ed.*, 2007, **46**, 4073.

Open Access Article. Published on 02 April 2015. Downloaded on 4/3/2026 6:59:41 AM.
This article is licensed under a Creative Commons Attribution 3.0 Unported Licence.

25 J. R. Carruthers, K. Prout and F. J. C. Rossotti, *Acta Crystallogr., Sect. B: Struct. Crystallogr. Cryst. Chem.*, 1975, **31**, 2044.

26 B. F. Hoskins, R. Robson and P. Smith, *J. Chem. Soc., Chem. Commun.*, 1990, 488.

27 See for example: (*a*) S. T. Onions, S. L. Heath, D. J. Price, R. W. Harrington, W. Clegg and C. J. Matthews, *Angew. Chem., Int. Ed.*, 2004, **43**, 1814; (*b*) D. Dragancea, V. B. Arion, S. Shova, E. Rentschler and N. V. Gerbeleu, *Angew. Chem., Int. Ed.*, 2005, **44**, 7938; (*c*) J. Xaio, B. Y. Liu, G. Wei and X. C. Huang, *Inorg. Chem.*, 2011, **50**, 11032; (*d*) X. C. Huang, J. P. Zhang and X. M. Chen, *J. Am. Chem. Soc.*, 2004, **126**, 31218.

28 See for example: (*a*) J. Schnack, *Dalton Trans.*, 2010, **39**, 4677; (*b*) J. Schnack, H. J. Schmidt, J. Richter and J. Schulenburg, *Eur. Phys. J. B*, 2001, **24**, 475; (*c*) I. Rousochatzakis, A. M. Lauchli and F. Mila, *Phys. Rev. B: Condens. Matter*, 2008, **77**, 094420; (*d*) J. Schnack and R. Schnalle, *Polyhedron*, 2009, **28**, 1620.

29 See for example: (*a*) J. Jaklič and P. Prelovšek, *Phys. Rev. B: Condens. Matter*, 1994, **49**, 5065; (*b*) J. Schnack and O. Wendland, *Eur. Phys. J. B*, 2010, **78**, 535; (*c*) J. Schnack, P. Hage and H.-J. Schmidt, *J. Comput. Phys.*, 2008, **227**, 4512.

30 S. Piligkos, *ITO-MAGFIT*, Department of Chemistry, University of Copenhagen, 2010.

31 A. Bencini and D. Gatteschi, *Electron Paramagnetic Resonance of Exchange Coupled Systems*, Springer, Heidelberg, 1990.

32 See for example: (*a*) D. Gaynor, Z. A. Starivoka, S. Ostrovsky, W. Haase and K. B. Nolan, *Chem. Commun.*, 2002, 506; (*b*) H. Saarinen, M. Orama and J. Korvenranta, *Acta Chem., Scand.*, 1989, **43**, 834.

33 See for example: (*a*) A. Escuer, G. Vlahopoulou, S. P. Perlepes and F. A. Mautner, *Inorg. Chem.*, 2011, **50**, 2468; (*b*) P. Chaudhuri, *Coord. Chem. Rev.*, 2003, **43**, 143; (*c*) C. J. Milios, T. C. Stamatatos and S. P. Perlepes, *Polyhedron*, 2006, **25**, 134; (*d*) P. A. Angardis, P. Baran, R. Boca, F. Cervantes-Lee, W. Haase, G. Mezei, R. G. Raptis and R. Werner, *Inorg. Chem.*, 2002, **41**, 2219.

34 See for example: (*a*) H. L. Zhu, C. X. Ren and X. M. Chen, *J. Coord. Chem.*, 2002, **55**, 667; (*b*) G. A. V. Albada, I. Mutikainen, U. Turpeinen and J. Reedijk, *Polyhedron*, 2004, **23**, 993; (*c*) M. Gonzalez-Alvarez, G. Alzuet, J. Borras, S. Garcia-Granda and J. M. Montejo-Bernardo, *J. Inorg. Biochem.*, 2003, **96**, 443; (*d*) V. K. Bhardwai, N. Aliaga-Alcalde, M. Corbella and G. Hundal, *Inorg. Chim. Acta*, 2010, **97**, 363; (*e*) S. Munoz, J. Pons, J. Ros, M. Font-Bardia, C. A. Kilner and M. A. Halcrow, *Inorg. Chim. Acta*, 2011, **373**, 211; (*f*) M. Drillon, A. Grand and P. Rey, *Inorg. Chem.*, 1990, **29**, 771; (*g*) H. E. LeMay Jr., D. J. Hodgson, P. Preuttiangkura and L. J. Theriot, *J. Chem. Soc., Dalton Trans.*, 1979, 781.

35 See for example: (*a*) M. Sutradhar, T. R. Barman, J. Klanke, M. G. B. Drew and E. Rentschler, *Polyhedron*, 2013, **53**, 48; (*b*) E. S. Koumousi, C. P. Raptopoulou, S. P. Perlepes, A. Escuer and T. C. Stamatatos, *Polyhedron*, 2010, **29**, 204; (*c*) M. Maekawa, S. Kitigawa, Y. Nakao, S. Sakamoto, A. Yatani, W. Mori, S. Kashino and M. Munakata, *Inorg. Chim. Acta*, 1999, **20**, 293; (*d*) A. Yatani, M. Fujii, Y. Nakao, S. Kashino, M. Kinoshita, W. Mori and S. Suzuki, *Inorg. Chim. Acta*, 2001, **316**, 127; (*e*) Y. Song, X. T. Chen, C. G. Zheng, D. R. Zhu, X. Z. You and L. H. Weng, *Transition Met. Chem.*, 2001, **26**, 247; (*f*) A. Escuer, G. Vlahopoulo, S. P. Perlepes, M. Font-Bardia and T. Clavet, *Dalton Trans.*, 2011, **40**, 225; (*g*) J. P. Naskar, C. Biswas, B. Guhathakurta, N. Aliaga-Alcade, L. Lu and M. Zhu, *Polyhedron*, 2011, **30**, 2310; (*h*) V. Mathrubootham, A. W. Addison, K. T. Holman, E. Sinn and L. K. Thompson, *Dalton Trans.*, 2009, 8111; (*i*) P. Dhal, M. Nandy, D. Sadhukhan, E. Zangrando, G. Pilet, C. J. Gomez-Garica and S. Mitra, *Dalton Trans.*, 2013, **42**, 14545; (*j*) L. K. Das, M. G. B. Drew, C. Diaz and A. Ghosh, *Dalton Trans.*, 2014, **43**, 7589.

36 A. D. Becke, *J. Chem. Phys.*, 1993, **98**, 5648.

37 (*a*) A. Schafer, H. Horn and R. Ahlrichs, *J. Chem. Phys.*, 1992, **97**, 2571; (*b*) A. Schafer, C. Huber and R. Ahlrichs, *J. Chem. Phys.*, 1994, **100**, 5829.

38 M. J. Frisch, G. W. Trucks, H. B. Schlegel, G. E. Scuseria, M. A. Robb, J. R. Cheeseman, G. Scalmani, V. Barone, B. Mennucci, G. A. Petersson, H. Nakatsuji, M. Caricato, X. Li, H. P. Hratchian, A. F. Izmaylov, J. Bloino, G. Zheng, J. L. Sonnenberg, M. Hada, M. Ehara, K. Toyota, R. Fukuda, J. Hasegawa, M. Ishida, T. Nakajima, Y. Honda, O. Kitao, H. Nakai, T. Vreven, J. A. Montgomery Jr., J. E. Peralta, F. Ogliaro, M. Bearpark, J. J. Heyd, E. Brothers, K. N. Kudin, V. N. Staroverov, R. Kobayashi, J. Normand, K. Raghavachari, A. Rendell, J. C. Burant, S. S. Iyengar, J. Tomasi, M. Cossi, N. Rega, J. M. Millam, M. Klene, J. E. Knox, J. B. Cross, V. Bakken, C. Adamo, J. Jaramillo, R. Gomperts, R. E. Stratmann, O. Yazyev, A. J. Austin, R. Cammi, C. Pomelli, J. W. Ochterski, R. L. Martin, K. Morokuma, V. G. Zakrzewski, G. A. Voth, P. Salvador, J. J. Dannenberg, S. Dapprich, A. D. Daniels, O. Farkas, J. B. Foresman, J. V. Ortiz, J. Cioslowski and D. J. Fox, *GAUSSIAN 09 (Revision A.02)*, Gaussian, Inc., Wallingford, CT, 2009.

39 L. Noodleman, *J. Chem. Phys.*, 1981, **74**, 5737.

40 E. Ruiz, S. Alvarez, A. Rodriguez-Fortea, P. Alemany, Y. Pouillon and C. Massobrio, in *Magnetism: Molecules to Materials*, ed. J. S. Miller and M. Drillon, Wiley-VCH, Weinheim, 2001, vol. II, p. 227.

41 T. Cauchy, E. Ruiz and S. Alvarez, *J. Am. Chem. Soc.*, 2006, **128**, 15722.

42 N. Berg, T. Rajeshkumar, S. M. Taylor, E. K. Brechin, G. Rajaraman and L. F. Jones, *Chem. – Eur. J.*, 2012, **18**, 5906.

43 T. Rajeshkumar, H. V. Annadata, M. Evangelisti, S. K. Langley, N. F. Chilton, K. S. Murray and G. Rajaraman, *Inorg. Chem.*, 2015, **54**, 1661.

44 (*a*) E. Ruiz, P. Alemany, S. Alvarez and J. Cano, *Inorg. Chem.*, 1997, **36**, 3683; (*b*) T. Rajeshkumar,

 This journal is © The Royal Society of Chemistry 2015

H. V. Annadata, M. Evangelisti, S. K. Langley, N. F. Chilton, K. S. Murray and G. Rajaraman, *Inorg. Chem.*, 2015, **54**, 1661.

45 (*a*) E. Ruiz, P. Alemany, S. Alvarez and J. Cano, *Inorg. Chem.*, 1997, **36**, 3683; (*b*) E. Ruiz, S. Alvarez, A. Rodriguez-Fortea, P. Alemany, Y. Pouillon and C. Massobrio, in *Magnetism: Molecules to Materials II*, ed. J. S. Miller and M. Drillon, Wiley-VCH, Weinheim, 2001, p. 227.

Open Access Article. Published on 02 April 2015. Downloaded on 4/3/2026 6:59:41 AM.
This article is licensed under a Creative Commons Attribution 3.0 Unported Licence.